Density functional study of H–Fe vacancy interaction in bcc iron

2004 J. Phys.: Condens. Matter 16 6907

(http://iopscience.iop.org/0953-8984/16/39/023)

INSTITUTE OF PHYSICS PUBLISHING JOURNAL OF PHYSICS: CONDENSED MATTER

J. Phys.: Condens. Matter **16** (2004) 6907–6916 PII: S0953-8984(04)80099-7

Density functional study of H–Fe vacancy interaction in bcc iron

M Estela Pronsato, Carolina Pistonesi and Alfredo Juan[1]

Departamento de Física, Universidad Nacional del Sur, Avenida Alem 1253, 8000 Bahía Blanca, Argentina

E-mail: cajuan@criba.edu.ar

Received 29 April 2004, in final form 4 August 2004
Published 17 September 2004
Online at stacks.iop.org/JPhysCM/16/6907
doi:10.1088/0953-8984/16/39/023

Abstract

The Fe–H interaction in the vicinity of a vacancy in bcc iron was studied within the framework of the density functional theory and the findings compared with previous results obtained by semiempirical molecular orbital methods. Calculations were performed using an iron cluster containing 12 atoms and a vacancy. Geometry optimizations were performed to find the most stable positions for one and two hydrogen atoms.

Changes in the electronic structure of Fe atoms near the vacancy were analysed when one and two H atoms are added to the iron cluster. Fe atoms surrounding the vacancy weaken their bond when hydrogen is present. This is interpreted in terms of the formation of Fe–H bonds.

(Some figures in this article are in colour only in the electronic version)

1. Introduction

The presence of interstitial hydrogen in transition metals has a great influence on the physical properties of the metal. Severe embrittlement can be produced in many metals even by very small amounts of hydrogen [1]. However, there is not a complete understanding of the hydrogen embrittlement mechanism. Lattice imperfections play a very important role in H–metal interaction; Myers *et al* provide an interpretation for the microscopic mechanisms involved in the interaction and consider the effects of hydrogen accumulation in microfissures, vacancies, dislocations and stacking faults, producing expansion and distortion of the metal lattice [2].

Both experimental and theoretical studies have been carried out regarding gas–metal interactions at surfaces, diffusion and absorption to bulk iron and trapping of hydrogen at defects [3–6].

[1] Author to whom any correspondence should be addressed.

Oriani [7] has suggested that some of the diffused hydrogen can be captured by lattice traps. Griessen [8] has developed a local semiempirical model capable of reproducing the measured energy of binding of hydrogen to vacancies and explains the trends of interstitial site occupancy of hydrogen in transition metals. Itsumi and Ellis [9] concluded that hydrogen localized in octahedral and tetrahedral interstitial sites near a vacancy weakens the nearest Fe–Fe bond.

The Fe–H interaction in the bulk of bcc iron near a vacancy has been studied in previous work by our group [10, 11]. Pistonesi *et al* [10] studied the electronic structure and bonding of a H–H pair in the vicinity of a bcc Fe bulk vacancy using the semiempirical atom superposition and electron delocalization molecular orbital method (ASED-MO) [12, 13].

Recently, Tateyama and Ohno investigated the stability of hydrogen–monovacancy complexes and their binding preferences in α-Fe by means of *ab initio* supercell calculations. They give theoretical evidence of hydrogen-enhanced vacancy formation in α-Fe [14].

In this work we continue the study of H absorption near an Fe vacancy using a density functional method (DFT).

2. Computational method

Gradient-corrected density functional theory (GC-DFT) calculations [15–17] were performed on a pure iron cluster containing 12 atoms, and on the cluster with one and with two hydrogen atoms, using the Amsterdam Density Functional 2000 package (ADF2000) [18]. The molecular orbitals were represented as linear combinations of Slater functions.

For the gradient correction the Becke [19] approximation for the exchange energy functional and the LYP [20] approximation for the correlation functional were employed.

In order to increase the computational efficiency, the internal atomic layers are kept frozen for every atom except hydrogen, since the internal electrons do not contribute significantly to the bonding. The frozen orbitals included up to Fe 3p. A basis set of triple-ζ quality was used (this means three Slater-type functions for each atomic valence orbital occupied).

To understand the H–Fe interaction we used the concepts of DOS (density of states) and COOP (crystal orbital overlap population) curves. The DOS curve is a plot of the number of orbitals per unit energy. The COOP curve is a plot of the overlap population weighted DOS versus energy. The integration of the COOP curve up to the Fermi level (E_F) gives the total overlap population of the bond specified and it is a measure of the bond strength.

3. Cluster model

In order to simulate the crystalline structure of bcc iron with and without a vacancy, cluster models were used. This cluster must have high symmetry, to save computational time, and at the same time it has to represent correctly the presence of the defect. It is a compromise between the computational efficiency and the realistic modelling of the bcc structure.

The cluster used to simulate the bcc solid iron is composed of 13 atoms, nine atoms belonging to a unit cell (eight occupying the vertices and one at the centre of a cube) and four more atoms corresponding to the centres of adjacent cells. Figure 1(a) shows three adjacent cells where the atoms forming the cluster are indicated. Increasing the size of the cluster up to 17 Fe atoms, considering the six adjacent cells, does not improve the results while making it more difficult to achieve numerical convergence. Dominguez *et al* [21] have shown that larger clusters do not always improve the calculation of electronic properties of the crystalline surface.

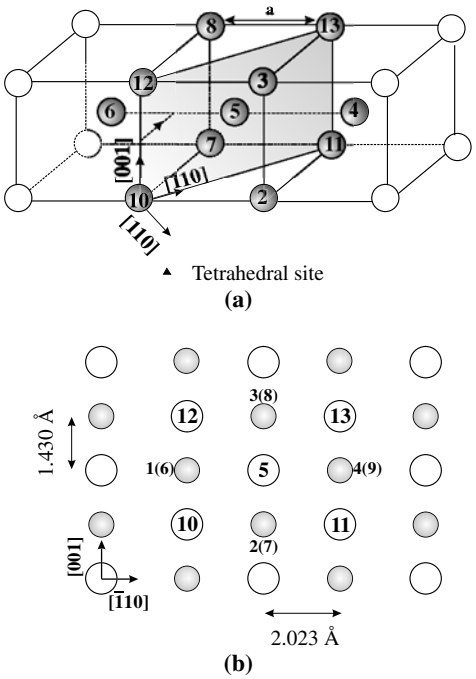

Figure 1. A bcc iron cluster containing 13 atoms. The darker circles represent 11 of the 13 iron atoms which form the cluster (a). (110) planes (b).

The small triangle in figure 1(a) indicates one of the tetrahedral interstitial sites of the cluster. This site is in the centre of a tetrahedron formed by atoms Fe_5, Fe_6, Fe_{10} and Fe_{12}. It is not a regular tetrahedron since four sides have a distance of $a\sqrt{3}/2$ (2.48 Å), where a is the lattice parameter, while the other two have a distance of a (2.861 Å). There are eight such tetrahedral interstitial sites in the cluster.

The atomic array of the (110) planes is shown in figure 1(b). The atoms forming the cluster are also indicated. Note that atoms Fe_1 and Fe_9 are not shown in figure 1(a).

Figure 2 shows the atomic array of (001) planes for a bcc structure and every tetrahedral interstitial site of the cluster which could be possible locations for H atoms.

The vacancy was simulated keeping the symmetry, by removing atom Fe_5 from the centre of the cluster.

4. Geometry optimization

4.1. H near the vacancy

We looked for the position of the hydrogen atom which minimizes the total energy of the cluster with the vacancy. The H atom was placed initially in one of the tetrahedral interstitial sites (T1 in figure 2) and allowed to perform small displacements in different directions. The geometry was optimized until the change in the energy gradient and in the Cartesian coordinates were 0.001 Hartree $Å^{-1}$ and 0.01 Å respectively.

The optimized position for the H atom was found near the tetrahedral site, but displaced 0.36 Å towards the vacancy, as shown in figure 3. This corresponds to a H–Fe distance of 1.77 Å from Fe_{10} and Fe_{12} and 1.62 Å from Fe_6, which are their first neighbours, and a

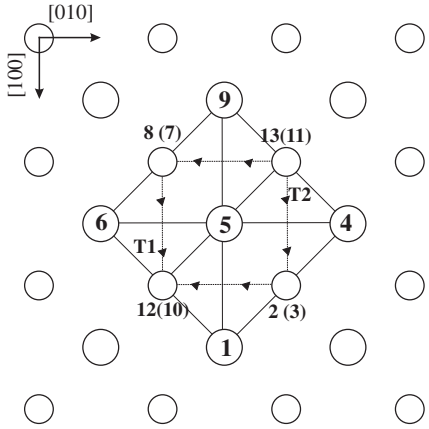

Figure 2. A view of a cluster (001) plane. Circles of different sizes indicate atoms belonging to different planes.

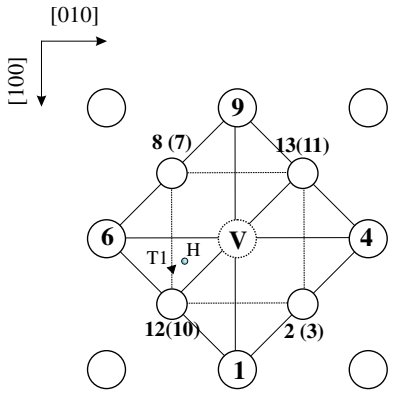

Figure 3. The position of the hydrogen atom after geometry optimization.

distance of 1.33 Å from the centre of the vacancy. To confirm that the geometry obtained was a true minimum in energy, a vibrational analysis was performed. We obtained real frequencies, indicating a minimum in energy instead of a saddle point in the energy surface. The absorption energy for the hydrogen atom (taken as the difference between the total energy of the Fe–H system and the energy of the Fe system and H separately) for that configuration was -1.76 eV. A negative absorption energy corresponds to a stabilized system.

The binding energy of H to the cluster with the vacancy is calculated as the difference between the energy of a H atom in its most favourable position in the metal without the vacancy (tetrahedral interstitial sites for bcc Fe) and the H atom trapped in the vacancy. The binding energy of the H atom to the vacancy obtained was 0.68 eV, a little higher than the experimental value, 0.53 eV. The semiempirical value obtained by Griessen was 0.78 eV [8]. The energy of binding of hydrogen to a vacancy obtained employing the ASED-MO method [10] was 0.17 eV.

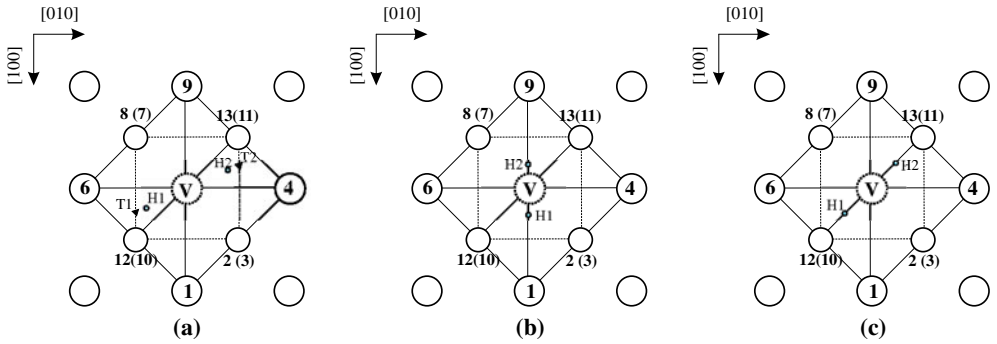

Figure 4. The location of two hydrogen atoms after geometry optimization when the initial positions are: (a) two tetrahedral interstitial sites; (b) sites located near the vacancy along direction [100] separated by 1 Å from each other; and (c) sites located near the vacancy along direction [110] separated by 0.85 Å from each other.

4.2. H–H pair near the vacancy

Before computing the absorption energy of a H–H pair near a vacancy in bcc Fe, a geometry optimization of the cluster was carried out. In the initial configuration for the optimization the H atoms were located in tetrahedral interstitial sites. Now both H atoms were allowed to perform small displacements in different directions. The choice of the tetrahedral sites was made considering the maximum symmetry possible for the cluster to reduce computational time. The sites chosen are indicated as T1 and T2 in figure 2.

We have also considered H location far from tetrahedral interstitial sites. Two other geometry optimizations were carried out with two different initial configurations where the H atoms were placed closer to the vacancy and separated at smaller distances from each other. Figure 4 shows H atom positions for all three cases studied.

Once the optimized geometry of the cluster was obtained, a vibrational analysis was performed in order to determine whether the configurations correspond to a true minimum in energy. In all cases a set of real frequencies was obtained.

Of the three cases studied, the configuration resulting from the first geometry optimization was the one with the minimum energy. In that configuration, the hydrogen atoms are shifted 0.28 Å from the tetrahedral positions towards the vacancy. The distance between the H atoms and their first Fe neighbours is 1.68 Å. The H–H distance was 2.69 Å. A similar result was obtained by Pistonesi *et al* using the ASED-MO method for an iron cluster containing 86 atoms with a vacancy [10]. They evaluated the hydrogen atom energy on a region surrounding the vacancy, to obtain a detailed energy surface. The energy minimum indicating the most stable positions for hydrogen atoms was found at tetrahedral interstitial sites but shifted about 0.20 Å towards the vacancy.

The absorption energy of the H–H pair in the cluster with a vacancy was obtained for the H atoms located in their optimized positions. It was calculated as the difference between the total energy of the iron cluster containing the H–H pair and the energy of cluster and H atoms far away from the solid surface. The energy obtained for the pair was -3.35 eV. The pair distance is considerable, so we expect no major interaction between H atoms and a prevailing Fe–H interaction. The pairing energy is positive ($1.76\ \text{eV} \times 2 > 3.35\ \text{eV}$), so no H–H pair is stabilized within the vacancy.

Table 1. Electronic densities for different atoms in the cluster.

		Orbital population			
	Spin density	s	p	d	OP
Without H					
Fe_6/Fe_4	3.115	0.850	0.448	6.790	
Fe_{10}/Fe_{11}	3.442	0.860	0.430	6.654	0.0339[a]
With H					
Fe_4	3.104	0.837	0.440	6.800	0.0049[b]
Fe_6	3.126	0.835	0.433	6.784	0.1262[c]
Fe_{10}	3.223	0.859	0.443	6.724	0.0243[a]
Fe_{11}	3.424	0.865	0.421	6.663	0.0333[d]
H_1	−0.064	0.790			
With 2H					
Fe_6/Fe_4	3.111	0.822	0.433	6.778	0.0995[b,e]
Fe_{10}/Fe_{11}	3.154	0.847	0.447	6.743	0.0214[a,d]
H_1/H_2	−0.056	0.805			0.0025[f]

[a] Fe_{10}–Fe_{12}.
[b] H_1–Fe_4.
[c] H_1–Fe_6.
[d] Fe_{11}–Fe_{13}.
[e] H_2–Fe_4.
[f] H_1–H_2.

5. Electronic structure analysis

Energy calculations for different spin polarization were carried out. It was found that the most stable configuration has a spin polarization of 3 μ_B/atom for the cluster without a defect and 3.3 μ_B/atom for the cluster containing a vacancy. Castro, using first-principles calculations and Fe clusters of different sizes, found that the magnetic momentum converges to a value of approximately 3 μ_B [22].

5.1. H near the vacancy

Introducing a H atom into the iron cluster cause a rearrangement of the orbital populations of iron. The most affected atom is Fe_6, the first neighbour to H. The s orbital population decreases from 0.850 to 0.835, while orbitals p and d do not change noticeably. Table 1 presents the electronic populations for different atoms in the cluster before and after introducing the hydrogen atoms.

It must be noticed that atoms Fe_{10} and Fe_{12} occupy equivalent positions inside the cluster as well as pairs: Fe_2–Fe_3; Fe_7–Fe_8; and Fe_{11}–Fe_{13} (see figure 2).

Figure 5 shows total DOS curves for the iron cluster with a vacancy and a hydrogen atom, located at its most stable position, and the projected DOS on the H atom and on the hydrogen first Fe neighbour. The small peak observed in the low energy region in figure 5(a) corresponds to orbital H 1s, since it matches in energy the projection of the H s states. Its contribution to the total density of states is larger than that found for the cluster containing 86 iron atoms with the ASED method [11]. This is due to the fact that the cluster studied in this work contains fewer atoms and the relative contribution of H is higher (1/12 versus 1/86). The peak is also observed in the projected DOS on the Fe first neighbours to H (Fe_6 and Fe_{10}), indicating a strong interaction with the metal. The peak is contributed mainly by 4s and 4d states with a

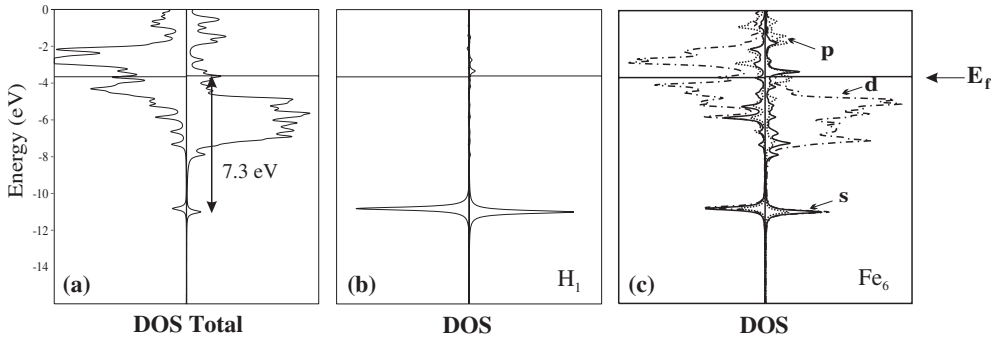

Figure 5. The total DOS for the H–Fe system (a); the projected DOS on H_1 (b) and the projected DOS on Fe_6 (c). DOS curves for different spin polarizations are shown separately.

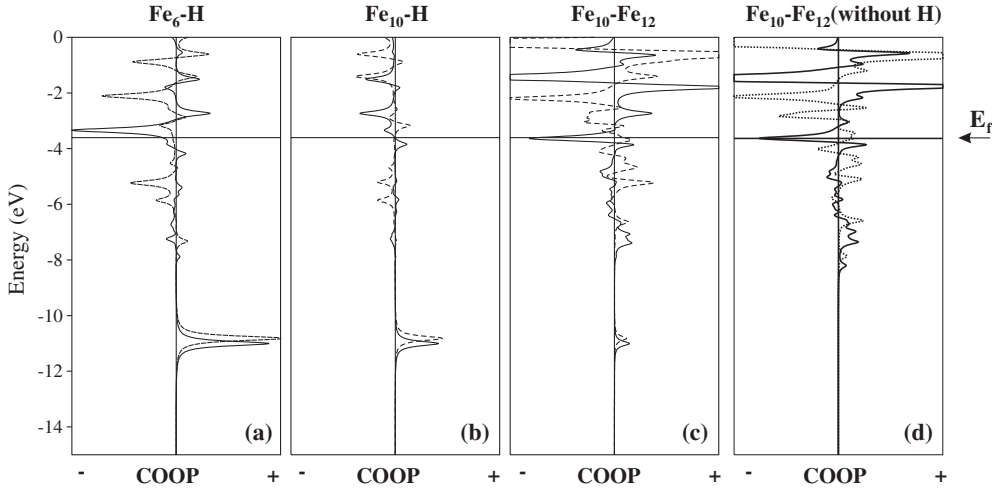

Figure 6. COOP curves for: (a) H–Fe_6; (b) H–Fe_{10}; (c) Fe_{10}–Fe_{12} when a hydrogen atom is present; and (d) Fe_{10}–Fe_{12} for the cluster without H. The solid and dotted curves correspond to different spin polarizations.

minor contribution from orbitals 3p of Fe. The interaction is negligible for Fe atoms at large distances from the H atom.

The DOS curve plots are similar to those obtained with the ASED-MO method but are shifted in energy. The energy of the highest occupied state was -3.66 eV. The peak corresponding to the hydrogen states is at -10.96 eV which is approximately 4.5 eV larger than the value calculated with the ASED-MO method [11]. However, the location of the peak relative to the Fermi level is the same as that obtained employing the ASED-MO method ($\widetilde{=}$7.3 eV).

The bonding study was performed analysing the overlap population of crystalline orbitals (COOP curves). In figure 6, COOP curves are shown for the interaction between H and its closest neighbour (Fe_6) and for the interactions between two Fe atoms (Fe_{10} and Fe_{12}) before and after the introduction of the hydrogen atom.

A bonding peak is observed for the Fe–H interaction and antibonding peaks lying above the Fermi level are also present. This gives a net bonding overlap population of 0.126

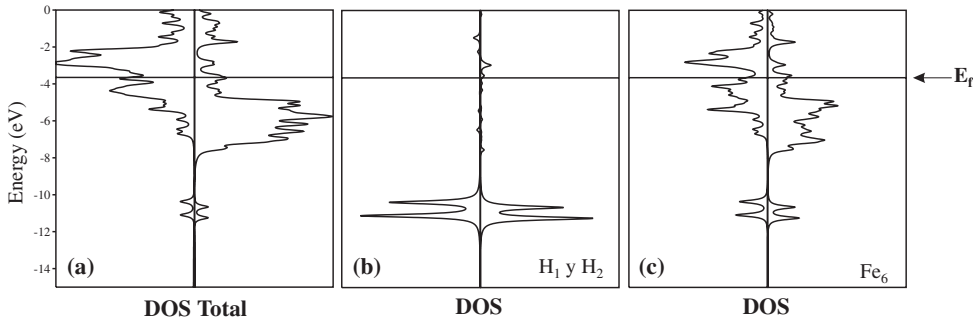

Figure 7. The total DOS for the iron cluster containing 12 atoms and a vacancy with two hydrogens (a) and the projected DOS on H_1 and H_2 (b) and that on Fe_6 (c). DOS curves for different spin polarizations are shown separately.

(see table 1). For the Fe–Fe interaction, it is observed that more antibonding states are filled when hydrogen is present. This makes the overlap population of atoms Fe_{10} and Fe_{12} decrease from 0.0339 to 0.0243, that is by 28%, which leads to a weakening in the iron–iron bond.

5.2. H–H pair near the vacancy

An electronic structure analysis was carried out for the minimum energy configuration found previously for the iron cluster with a vacancy containing the H–H pair. The H atoms are separated a distance of 2.69 Å from each other and are 1.68 Å away from their first Fe neighbours.

In the total DOS curves two peaks are observed corresponding to H states. There is little interaction between the H atoms due to the large distance between them. For that reason there is almost no separation between the peaks which lie almost at the same energy value (see figure 7), indicating the lack of H–H association and the mere existence of two isolated H atoms.

Due to the introduction of another hydrogen, now the populations of s and d states of atoms Fe_4, Fe_{11} and Fe_{13} decrease in a similar way to how those of Fe_6, Fe_{10} and Fe_{12} had, after the first H was introduced (see table 1).

COOP curves are shown in figure 8 for H–H, Fe–H and Fe–Fe interactions. There is no bonding interaction between the two hydrogen atoms due to the large separation. On the other hand, bonding peaks are observed for each H atom and their first Fe neighbours. Each H affects its closest Fe in the same way, forming an Fe–H bond and weakening the existing Fe–Fe bond. The overlap population of Fe_{11} and Fe_{13}, which had not been affected by the introduction of H_1, now decreases from 0.0333 to 0.0214 (35%).

6. Vibrational analysis

A vibrational analysis was performed for the cluster with one hydrogen located near a vacancy at its most stable position. The frequency of vibration values were calculated for H displacements in directions $[\bar{1}10]$, [110] and [001]. The displacement amplitude was 0.01 Å. The calculated frequencies were 500 and 568 cm^{-1} for the normal modes along $[\bar{1}10]$ and [001] respectively and 1290 cm^{-1} for the normal mode along [110].

Cremaschi *et al* [23], studying chemisorption of H on Fe (110) with *ab initio* methods, calculated the tension frequency of vibration of the H surface. They found that for long

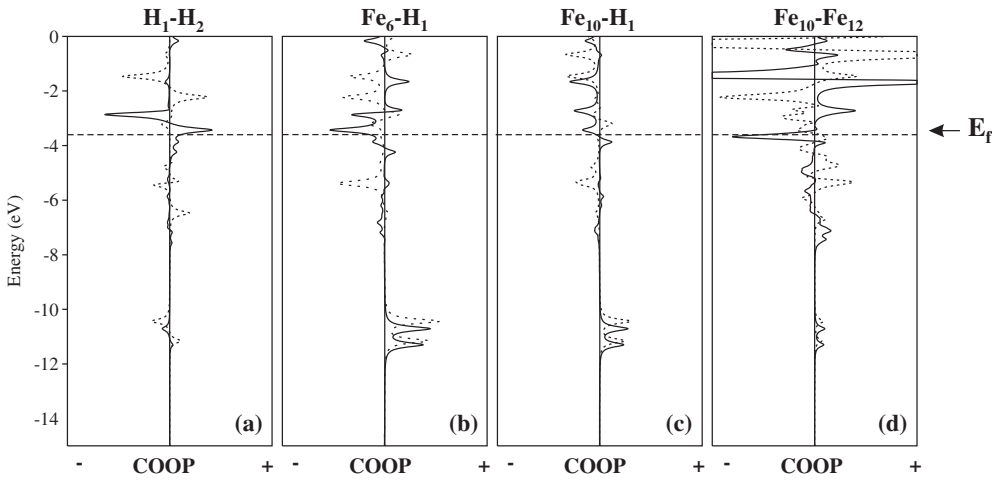

Figure 8. COOP curves for: H_1–H_2 (a); H_1–Fe_6 (b); H_1–Fe_{10} (c); and Fe_{10}–Fe_{12} (d). The solid and dotted curves correspond to different spin polarizations.

bridge, short bridge, and quasi-tricoordinated sites, the frequencies were 1070, 1066 and 1073 cm^{-1} respectively. For each case the calculated Fe–H distances were 1.69, 1.61 and 1.74 Å respectively.

7. Conclusion

The hydrogen–iron interaction was studied for an iron cluster containing 12 atoms with a vacancy, by means of density functional theory within the non-local approximation. The main features of the Fe–H interaction agree with results obtained with the semiempirical ASED-MO method for larger clusters.

The most stable configuration is obtained with a spin polarization of 3 μ_B/atom for the perfect cluster and 3.3 μ_B/atom for the cluster with a vacancy.

The geometry of the cluster was optimized for the cluster with one and two hydrogen atoms. Due to the introduction of the H atoms there is a decrease in the population of s and p states of iron atoms closest to the hydrogen atoms.

The H atoms do not bond with each other but they bond with their closest Fe atoms, weakening the existing Fe–Fe bonds.

Acknowledgments

Our work was supported by CONICET, Fundación Antorchas, Departamento de Física UNS and ANPCyT (PICT 12-09857). We thank the referees for valuable comments.

References

[1] Bernstein I M and Thompson A W 1981 *Hydrogen Effects in Metals* (Warrendale, PA: American Institute of Metals)

[2] Myers S M, Baskes M I, Birnbaum H K, Corbett J W, De Leo G G, Estreicher S K, Haller E E, Jena P, Johnson N M, Kirchheim R, Pearton S J and Stavola M J 1992 *Rev. Mod. Phys.* **64** 559–617

[3] Chorkendorff I, Russell J N Jr and Yates J T Jr 1987 *Surf. Sci.* **182** 375–89

[4] Irigoyen B, Ferullo R, Castellani N and Juan A 1995 *Modelling Simul. Mater. Sci. Eng.* **3** 319–29
[5] Irigoyen B, Ferullo R, Castellani N and Juan A 1996 *J. Phys. D: Appl. Phys.* **29** 1306–9
[6] Juan A and Pistonesi C 1998 *Mater. Chem. Phys.* **55** 61–7
[7] Oriani R A 1970 *Acta Metall.* **18** 147–57
[8] Griessen R 1988 *Phys. Rev.* B **38** 3690–8
[9] Itsumi Y and Ellis D E 1996 *J. Mater. Res.* **11** 2206–13
[10] Pistonesi C, García A J, Brizuela G and Juan A 1998 *J. Phys. D: Appl. Phys.* **31** 588–94
[11] Juan A, Pistonesi C, García A J and Brizuela G 2003 *Int. J. Hydrog. Energy* **28** 995–1004
[12] Hoffmann R and Lipscom W N 1962 *J. Chem. Phys.* **36** 2179–89
[13] Anderson A B and Hoffmann R 1974 *J. Chem. Phys.* **60** 4271–3
[14] Tateyama Y and Ohno T 2003 *Phys. Rev.* B **67** 174105–15
[15] Hohenberg P and Kohn W 1964 *Phys. Rev.* B **136** 864–71
[16] Kohn W and Sham L J 1965 *Phys. Rev.* B **140** 1133–8
[17] Parr R G and Yang W 1989 *Density Functional Theory of Atoms and Molecules* (New York: Oxford University Press)
[18] *Amsterdam Density Functional Package* Release 2000.1, Vrije Universiteit, Amsterdam
[19] Becke D 1988 *Phys. Rev.* A **38** 3098–100
[20] Lee C, Yang W and Parr R G 1988 *Phys. Rev.* B **37** 785–9
[21] Domínguez-Ariza D, Sousa C, Harrison N M, Ganduglia-Pirovano M V and Illas F 2003 *Surf. Sci.* **522** 185–97
[22] Castro M 1997 *Int. J. Quantum Chem.* **64** 223–30
[23] Cremaschi P, Yang H and Whitten J L 1995 *Surf. Sci.* **330** 255–64